Fabrication of gas-diffusion electrodes at various pressures and investigation of synergetic effects of mixed electrocatalysts on oxygen reduction reaction

Hussien Gharibi[*], Rasol Abdullah Mirzaie

Department of Chemistry, Faculty of Science, Tarbiat Modarres University, P.O. Box 14115-175, Tehran, Iran

Abstract

This work introduces a new method for the construction of gas-diffusion electrodes (GDEs) for fuel cells. Sampled dc voltammetry is used to study the oxygen reduction reaction (ORR) during the rate-determining step. In this study, GDEs are fabricated in two separate stages: pressure processing followed by temperature processing. The GDE that gives the best performance is constructed at a pressure of 60 kF cm^{-2}, and has a platinum loading of 0.5 mg cm^{-2} and 30% polytetra fluoroethylene (PTFE) in the reaction layer. The values of the symmetry factor and exchange current density of this optimal GDE are 0.5279 and 35.16 mA cm^{-2}, respectively. In order to reduce or eliminate the polarization effect, two types of electrocatalyst (platinum on carbon and platinum on activated charcoal) with different surface areas are combined to create a mixed electrocatalyst. An investigation is made of the electrochemical characteristics of pure samples of each electrocatalyst and mixtures of the two electrocatalysts over a range of mole ratios. The results indicate that, under optimized conditions (a platinum loading of 0.9 mg cm^{-2} with a mole fraction of platinum on carbon of 0.8), the exchange current density is 92.55 mA cm^{-2}. The use of a mixed electrocatalyst reduces the concentration polarization of the ORR in the rate-determining step.
© 2003 Elsevier Science B.V. All rights reserved.

Keywords: Fuel cells; Gas-diffusion electrode; Oxygen reduction reaction; Synergetic effect; Mixed electrocatalyst

1. Introduction

Currently, a variety of fuel cells are in different stages of development. They can be classified into diverse categories according to the type of fuel and oxidant, whether the fuel is processed inside (internal reforming) or outside (external reforming) the fuel cell, the type of electrolyte, the temperature of operation, whether the reactants are fed into the cells by internal or external manifolds, etc. The operating temperature and useful life of the fuel cell dictate the physicochemical and thermomechanical properties of the materials used in the cell components. The capabilities of proton exchange membrane (PEM) fuel cells rely on their simplicity. In PEM fuel cells, the electrolyte is a solid polymer which contains mobile protons. The performance of PEM cells depends on the electrochemical properties of the cell elements. The electricity production capability of PEM fuel cells is depends on the performance of gas-diffusion electrodes [1,2].

The cathode electrode consists of an electrode support and an electrocatalyst layer. The electrode support is made from porous carbon paper, while the electrocatalyst layer consists of platinum-dispersed carbon powders which are joined by polytetra fluoroethylene (PTFE) particles. Like the electrode support, the electrocatalyst layer is also porous to gases. The electrode support supplies reactant gases such as hydrogen and oxygen to the electrocatalyst layer; the electrochemical reactions occur in the electrocatalyst layer [3].

The performance of fuel-cell electrodes can be improved either by using a more active electrocatalyst or by improving the structure of the electrocatalyst so as to minimize transport losses and to increase the chances of simultaneous contact of gaseous reactant, catalyst and electrolyte [4]. Pt/C catalysts are widely used both in electrochemical power sources and in electrolysis. For example, gas-diffusion electrodes made from Pt/C catalysts are employed in fuel cells to reduce the quantity of noble metal used [5].

Many studies have reported synergistic properties for mixed systems such as mixed surfactants, physical mixture of catalyst, etc. [6–16]. Recent articles [17,18] suggest that hydrogen spillover [19–24] can be 'harnessed' to yield

* Corresponding author. Tel.: +98-21-646-2548; fax: +98-21-646-2254.
E-mail address: gharibi@irandoc.ac.ir (H. Gharibi).

highly active and selective catalysts. Spillover involves the transport of an active species sorbed or formed on a first phase to another phase on which the active species does not sorb or form under the same conditions. For example, hydrogen atoms generated by a noble metal can activate bond-shift type isomerization on a physically separated second surface. Specifically, kinetic studies in which FeCe/Grafoil was incrementally added to a bed which initially contained only Pt/Grafoil showed that the physical mixture is $10\times$ more active than the sum of the activities of the individual materials [25]. Indeed, it was found that each incremental addition of FeCe/Grafoil led to an increase in activity far larger ($100\times$) than that which would be anticipated based on the measured activity of FeCe/Grafoil in the absence of platinum. It was also shown that physical mixtures containing a graphite-supported 'alloy' (FeCe) and a graphite-supported noble metal (palladium or platinum) display synergism for butadiene hydrogenation/isomerization. That is, the activity of the mixtures is far higher than that anticipated from the addition of the activities measured for each material alone.

Electronic interactions and synergetic effects between the metal and the support in electrocatalytic systems have been demonstrated to be of primary importance in a fashion similar to heterogeneous catalysis [26]. Several studies have shown that the difference in work function between the metal and the support induces changes in the electronic state of the supported Pt, and that these changes account for the observed variations in electrocatalytic activity in these systems [27–29].

The electrochemical reduction of oxygen on platinum plays an important role in energy conversion since the associated overpotential corresponds to a voltage loss of 200–300 mV at operational current densities [30–40]. The influence of electrocatalyst characteristics on the activity and the stability of the oxygen reduction reaction in phosphoric acid fuel cells has been investigated [41–43].

In the present study, GDEs have been fabricated in which the electrocatalyst consists of a mixture of two types of electrocatalyst with different surface areas. Specifically, a mixture of platinum on carbon with high and low surface area is used. Such mixtures provide an opportunity to improve the cell performance compared with that of cells with a single carbon substrate. Various factors influence the performance of a GDE for the oxygen reduction reaction. In this work, three key factors are examined, namely: the amount of PTFE in the reaction layer, the pressure applied to compress the electrodes, and the synergetic effect of using a mixture of electrocatalyst.

2. Experimental

2.1. Fabrication of the gas-diffusion electrode

Commercially available cathode electrocatalysts were used to prepare the PTFE bonded porous GDE. Two electrocatalysts with different surface areas, 10% platinum on carbon (surface area 100 $m^2\ g^{-1}$) and 10% platinum on activated charcoal (surface area 900 $m^2\ g^{-1}$), were obtained from Electro Chem. and Merck, respectively. In this paper, platinum on carbon and platinum on activated charcoal electrocatalysts are referred to as PC and PAC, respectively. The catalyst dough was formed by mixing PTFE solution (Electro Chem.), distilled water and isopropyl alcohol (Aldrich 99%). Ultrasound was used to create a highly-dispersed mixture and the resulting dough was rolled to the desired size. The catalyst layer was bonded to 50% PTFE-loaded carbon papers, pressed by a hydraulic press, and sintered at 350 °C for 20 min under inert conditions.

2.2. Electrochemical studies of GDE

The oxygen reduction reaction was evaluated in the cathode by a new approach, in which the current density was measured with respect to potential using a half-cell measurement apparatus which comprised a three-electrode system. An Ag/AgCl electrode was employed as the reference electrode, a Pt electrode constructed from Pt plate was utilized as the counter electrode, and the GDE described above was used as the working electrode. The GDE contained catalyst and a gas-diffusion layer.

The GDE was set in a glass holder and then placed in sulfuric acid (3 mol dm^{-3}). In all experiments, oxygen gas was introduced into the holder under a pressure of 1 atm. The temperature of the was controlled by circulation of water at 333 K. The electrochemical behaviour of the GDEs was studied by means of sampled dc voltammetry using a potentiostat/galvanostat electrochemical measurement apparatus (EG&G, Model 273A).

The scanning rate, scan increment and step/drop time used in the experiments were 1 mV s^{-1}, 2 mV, and 2 s, respectively. The voltage was scanned from 0.7 to -0.2 V versus a Ag/AgCl electrode. Tafel plots were used to determine the symmetry factor (α) and exchange current density (i_0) at the rate-determining step.

2.3. Deterinination of α and i_0

In 1905, Tafel plotted overvoltage against log of current density and found that, for most values of the overvoltage, the graph approximates to a straight line. Such plots are now known 'Tafel plot'. Most values of the overvoltage, η, are given by the Tafel equation

$$\eta = \frac{2.3RT}{n\alpha F} \log \frac{i}{i_0} \tag{1}$$

where R is the gas constant; T the temperature, n the number of exchanged electrons; α the symmetry factor; i and i_0 the current density, and exchange current density respectively [44].

At zero exchange current density (i_0) no reaction can occur. This exchange current density is crucial to the control

of the performance of fuel-cell electrodes. It is vital to make the value of i_0 as high as possible. It is affected by several parameters other than the material used for the electrode. Increasing the value of i_0 reduces the voltage drop [4]. Exchange current densities are analogous to rate constants in chemical reactions. Unlike rate constants, however, current densities are concentration dependent. Variations due to concentration are not very significant when compared with the range of variations in the rate constants [45]. Tafel plots are used to determine the values of the symmetry factor (α) and i_0. The slope and intercept of a Tafel plot give α and i_0, respectively.

3. Results and discussion

3.1. Optimization of GDE fabrication pressure at a range of PTFE concentrations

To investigate the influence of pressure on the fabrication and structure of GDEs, were constructed at pressures of 400 and 60 kgF cm^{-2} with various PTFE concentrations. These electrodes are referred to below as high compressed GDE (HGDE) and low compressed GDE (LGDE), respectively. The final content of platinum in the reaction layer of cathode was 0.5 mg cm^{-2} in all cases.

3.1.1. Exchange current density
A plot of exchange current density versus PTFE concentration in the reaction layer is shown in Fig. 1. HGDE and LGDE give the highest exchange current densities at 50% PTFE and 30% PTFE, respectively, and the maximum exchange current density of the LGDE is higher than that of the HGDE. According to the data in Fig. 1, the oxygen reduction rate depends on both the concentration of PTFE and the fabrication pressure of the GDE.

3.1.2. E/i response
The current density versus PTFE percentage in the reaction layer at voltages of 300, 500 and 700 mV for the HGDE and LGDE are given in Figs. 2 and 3, respectively. At all
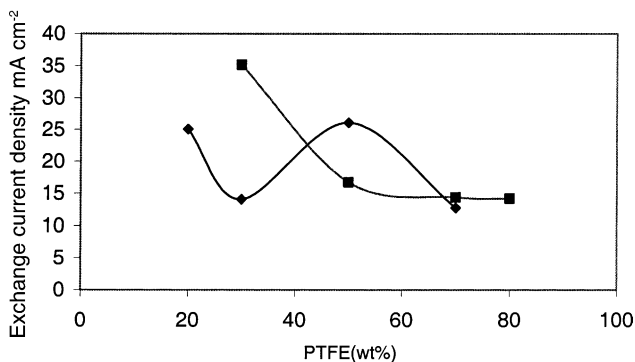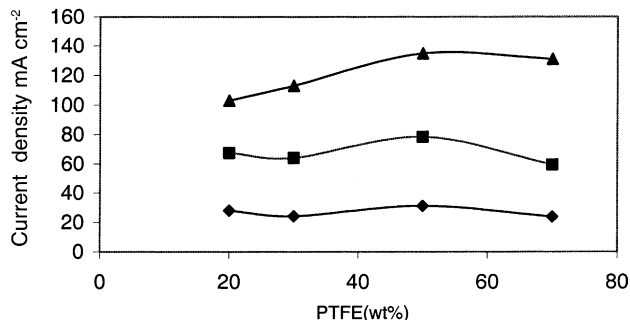
Fig. 2. Current density vs. PTFE content at 333 K at several voltages using HGDE: (◆), 700 mV; (■), 500 mV; (▲), 300 mV.
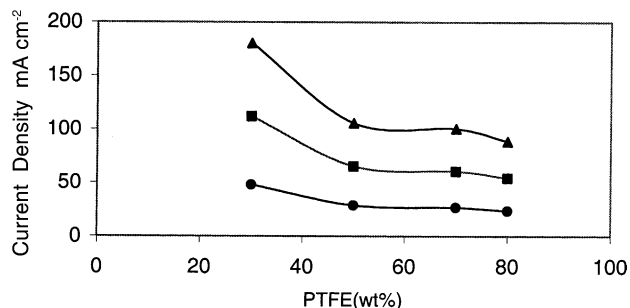
Fig. 3. Current density vs. PTFE content at 333 K at several voltages using LGDE: (◆), 700 mV; (■), 500 mV; (▲), 300 mV.

voltages, the highest value of the current density is observed at 50 and 30% PTFE for the HGDE and LGDE, respectively. Notably, both the HGDE and LGDE systems at 700 mV show very little variation in current density with increasing PTFE concentration. By contrast, the current density at 300 mV is strongly dependent on PTFE concentration because of mass transport. At high voltages, the process is controlled by electron transfer and by diffusion of the electroactive reactants.

3.1.3. Symmetry factor
The dependence of the symmetry factor on the PTFE concentration in the reaction layer for the HGDE and LGDE

Fig. 1. Exchange current density vs. PTFE content at 333 K: (◆), HGDE; (■), LGDE.
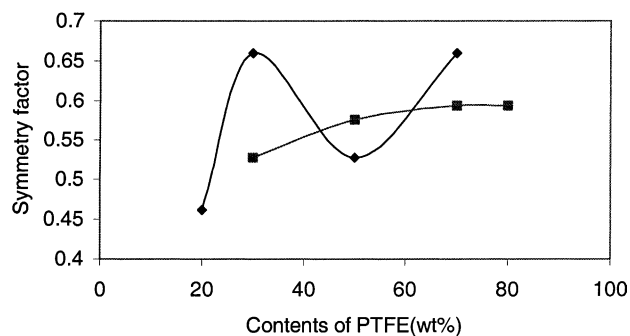
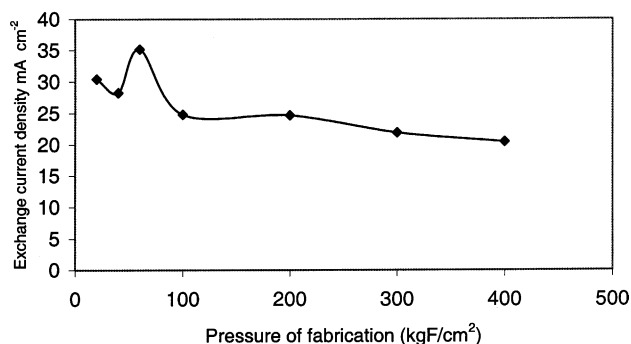Fig. 4. Symmetry factors vs. the PTFE content at 333 K: (◆), HGDE; (■), LGDE.

Fig. 5. Exchange current density vs. pressure of fabrication of electrodes at 333 K.

is shown in Fig. 4. For both electrodes, the symmetry factor is around 0.5. This indicates that the reaction is reversible rate-determining step. In practice, the cathodic and anodic current densities across the electrode with change of over-potential are symmetrical. The value of α is the proportion of the applied electrical energy that is harnessed in changing the rate of the electrochemical reaction. Its value depends on the reaction involved and the electrode material, but it must be in the range 0–1. For the hydrogen electrode, α is about 0.5 for a wide variety of electrode materials. The charge-transfer coefficient at the oxygen electrode shows greater variation, but is still between about 0.5 and 0.9 in most cases. For the electrodes studied here, the value of α varies between 0.45 and 0.65 depending on the amount of PTFE in the electrode. Taken together, our results indicate that the best performance is obtained for a system with 30% of PTFE in the LGDE.

3.2. Optimization of fabrication pressure for GDE containing 30% PTFE

3.2.1. Effect of GDE fabrication pressure on exchange current density of ORR

As shown in Fig. 5, the exchange current density varies with the pressure applied during electrode preparation for electrodes with 30% PTFE in the reaction layer. The highest value of the exchange current density is observed at $60 \, \text{kgF} \, \text{cm}^{-2}$. The exchange current density is approximately constant at pressures greater than $100 \, \text{kgF} \, \text{cm}^{-2}$, which suggests that the fabrication pressure of the GDE does not influence the rate of the ORR in this pressure region.

3.2.2. Effect of GDE fabrication pressure on E/i responses of ORR

The variation in current density with pressure applied during electrode preparation for voltages of 300, 500, and 700 mV is presented in Fig. 6. At all voltages, the maximum current density is at $60 \, \text{kgF} \, \text{cm}^{-2}$. The system at 300 mV has greater fluctuations of current density, and that this effect arises due to mass-transfer control of the ORR which, in turn, arises from high compression of pores.

3.2.3. Effect of GDE fabrication pressure on symmetry factor of ORR

The dependence of the symmetry factor, α, on the pressure used to fabricate the GDE with 30% PTFE is given in Fig. 7. The symmetry factor varies with increasing fabrication pressure in the low pressure region (40–$100 \, \text{kgF} \, \text{cm}^{-2}$), but remains almost constant at pressures greater than $100 \, \text{kgF} \, \text{cm}^{-2}$. The value is approximately 0.5 at all pressures applied during electrode preparation. These results indicate that the GDE with 30% PTFE gives the best performance when prepared at $60 \, \text{kgF} \, \text{cm}^{-2}$.

3.3. Synergetic effect of mixed electrocatalysts

To study the effect of synergism on ORR performance of GDEs, GDEs were prepared from a mixture of electrocatalysts which had carbon substrates with different surface areas, specifically, platinum electrocatalysts with surface areas of $100 \, \text{m}^2 \, \text{g}^{-1}$ (PC) and $900 \, \text{m}^2 \, \text{g}^{-1}$ (PAC). In the mixed electrocatalyst, the amount of platinum was varied from 0.3 to 1 mg cm^{-2} since the mole fractions of the mixed electrocatalyst was changed according to Fig. 8. The optimized pressure ($60 \, \text{kgF} \, \text{cm}^{-1}$) and PTFE content (30%) obtained from the experiments described in Sections 3.1
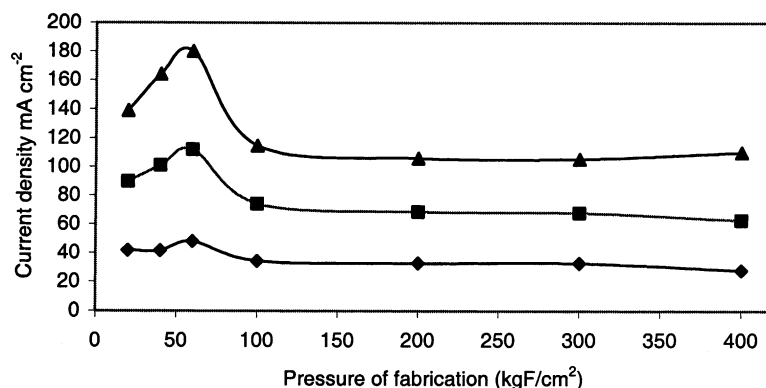

Fig. 6. Current density vs. pressure of fabrication of electrodes at 333 K at various voltages: (◆), 700 mV; (■), 500 mV; (▲), 300 mV.
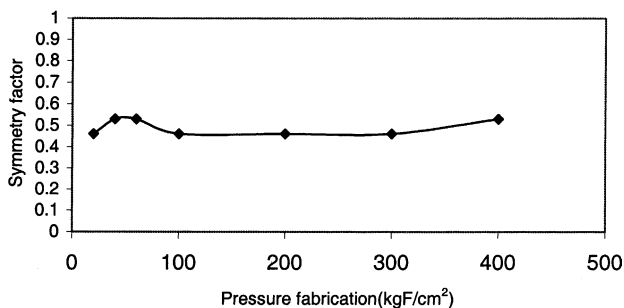
Fig. 7. Symmetry factors vs. pressure of fabrication of electrodes at 333 K.

and 3.2 were used in the fabrication of the mixed-catalyst GDEs.

3.3.1. Exchange current density

The exchange current density as a function of platinum concentration for GDEs made from either PC or PAC is shown in Fig. 9. For platinum loadings of 0.3–0.7 mg cm^{-2}, PC gives a higher current density than PAC. On further increase of the platinum loading, however, PAC gives a higher current density than PC. In Fig. 8, the exchange current density is plotted against the mole fraction of PC in the reaction layer. Here, the mole fraction is equal to 0 for

the composition layer free of PC, but equal to 1 for the composition layer free of PAC. Thus, the values of i_0 are based on two types of electrocatalysts, namely pure and mixed electrocatalyst.

3.3.1.1. Pure electrocatalyst.
As has been shown in Fig. 9, in the case of pure PC, the best GDE performance is obtained with a loading of 0.5 mg cm^{-2} of platinum. For pure PAC, the best and worst efficiency is observed for a loading of 0.3 and 1 mg cm^{-2}, respectively. This indicates that the ORR depends on both the composition and amount of platinum electrocatalyst in the reaction layer.

3.3.1.2. Mixed state.
In the system containing a mixture of PC and PAC, the ORR performance of the GDEs varied with the mole fraction of electrocatalyst for electrodes with the same loading of platinum. This indicates that the electrode efficiency is related to both the amount of platinum and the relative amounts of PC and PAC in the electrocatalyst. An increase in the loading of PC in the GDE reaction layer results in a decrease in GDE performance because of concentration overvoltage. The physical mixture of PC and PAC causes, however, a reduction in the concentration polarization of the ORR. It is considered that this reduction is the result of synergetic effects between the two
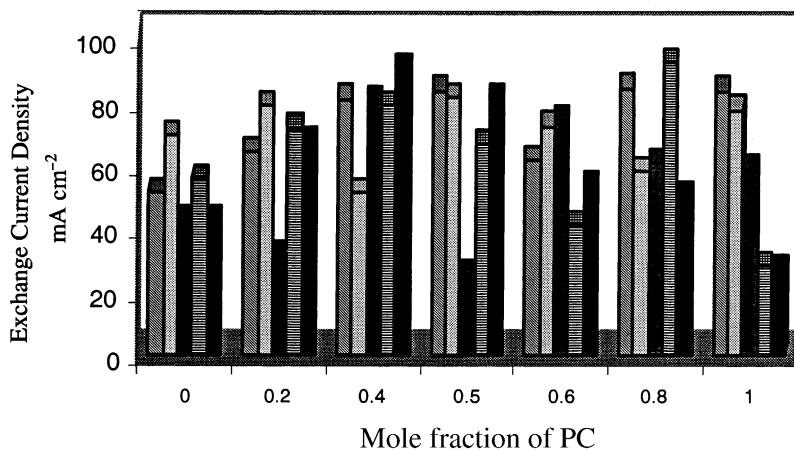

Fig. 8. Exchange current density vs. mole fraction of PC of platinum on carbon for various electrocatalyst loadings at 333 K: (▨), 0.3 mg cm^{-2}; (▧), 0.5 mg cm^{-2}; (▥), 0.7 mg cm^{-2}; (▤), 0.9 mg cm^{-2}; (■), 1 mg cm^{-2}.
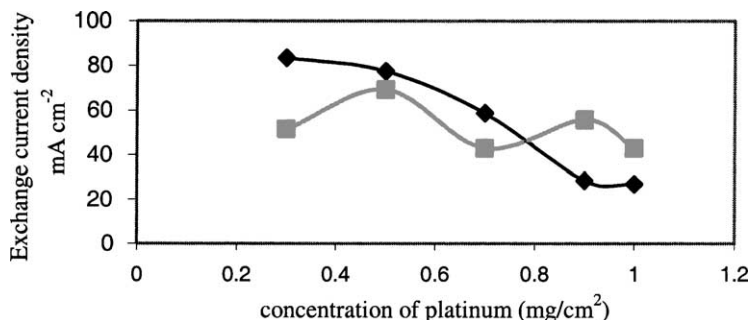

Fig. 9. Exchange current density vs. platinum concentration at 333 K: (◆), platinum on carbon; (■), platinum on activated charcoal.
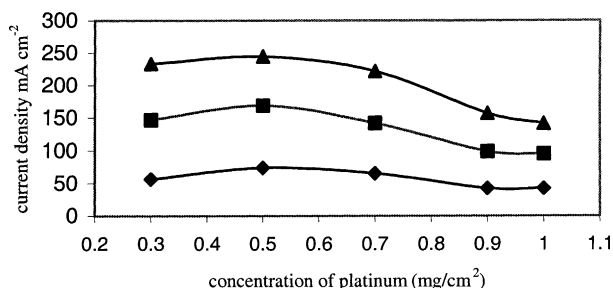
Fig. 10. Current density vs. concentration of platinum on carbon at 333 K at several voltages: (◆), 700 mV; (■), 500 mV; (▲), 300 mV.
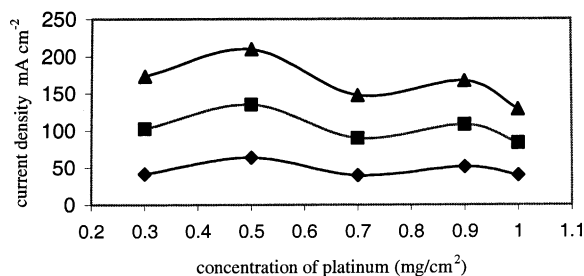

Fig. 11. Current density vs. concentration of platinum on charcoal active at 333 K at several voltages: (◆), 700 mV; (■), 500 mV; (▲), 300 mV.

components of the mixed electrocatalyst. For GDEs with 1 mg cm^{-2} platinum in the reaction layer, the best result is obtained at a mole fraction of 0.4. The exchange current density in this case is higher than that obtained with a 0.3 mg cm^{-2} loading of PC. The highest exchange current density is obtained for a platinum loading of 0.9 mg cm^{-2} since the mole fraction of PC is equal to 0.8. These results may be ascribed to synergetic effects of the electrocatalyst substrate (carbon and charcoal).

3.3.2. E/i response

The dependence of current density on platinum concentration for the pure PC and PAC systems, at voltages of 300, 500 and 700 mV is given in Figs. 10 and 11, respectively.

The optimal platinum loading is 0.5 mg cm^{-2} for both electrocatalysts in the pure state, but PC shows better efficiency (i.e. higher current density) in comparison with PAC. Of particular note is the fact that, contrary to the expectation that efficiency would monotonically increase with increasing platinum concentration, the experimental results indicate that a high platinum loading gives lower performance. At high platinum loadings, PAC performs better than PC due to its higher surface are. It should be emphasized that at high voltage (i.e. 700 mV), the change in current density is not too high, with increasing concentration of platinum over the range 0.3–1 mg/cm^2. At low voltage (300 mV), however the current density varies markedly because of the appearance of a concentration overvoltage.

Plots of current density versus mole fraction of PC of electrocatalyst for a constant amount of platinum in the reaction layer are presented in Figs. 12–16. These experiments have been done at various voltages include 300, 500 and 700 mV. The maximum point in each graph indicates the best efficiency of ORR at the rate-determining step. As earlier mentioned, at 700 mV the variation of mole fraction once again has little influence on the current density. On the other hand, at 300 mV the current density is strongly dependent on the composition of the reaction layer. The reason for this behaviour is that at low voltage mass transfer rather than heterogeneous kinetics restricts the current density. At a loading of 0.3 mg cm^{-2} of platinum (Fig. 12), the best performance is obtained using a mole fraction of PC of 0.8 for all of the voltages considered. For platinum loadings of 0.5, 0.7, 0.9 and 1 mg cm^{-2} (Figs. 13–16), the optimum mole fractions of PC are 0.5, 0.4, 0.8 and 0.4, respectively. The synergism effect is predominant at large amounts of platinum such as 0.9 and 1 mg cm^{-2} since the value of the current density is increased by factors of two at the rate-determining step of the ORR with respect to that for the pure state of either PC or PAC.

3.3.3. Symmetry factor

The dependence of the symmetry factor (α) on the concentration of platinum in pure PC and PAC is shown in
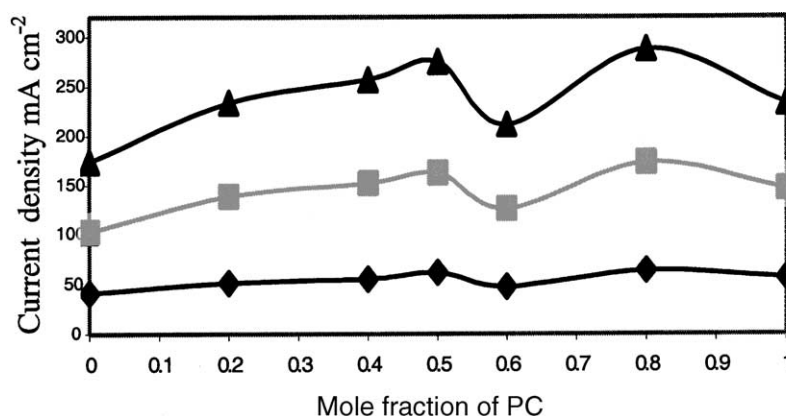

Fig. 12. Current density vs. mole fraction of PC at 333 K at several voltages using 0.3 mg cm^{-2} of platinum: (◆), 700 mV; (■), 500 mV; (▲), 300 mV.
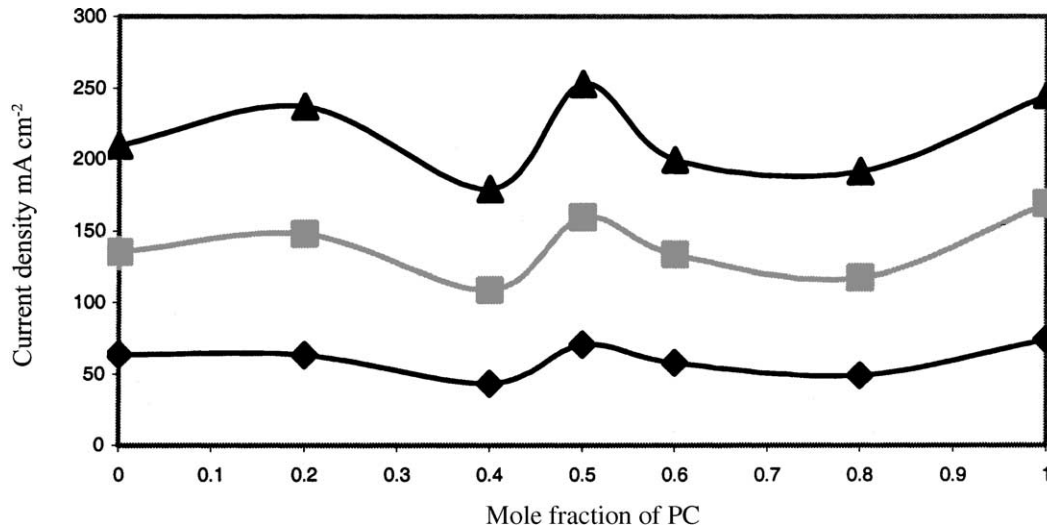
Fig. 13. Current density vs. mole fraction of PC at 333 K at several voltages using 0.5 mg cm^{-2} of platinum; (◆), 700 mV; (■), 500 mV; (▲), 300 mV.
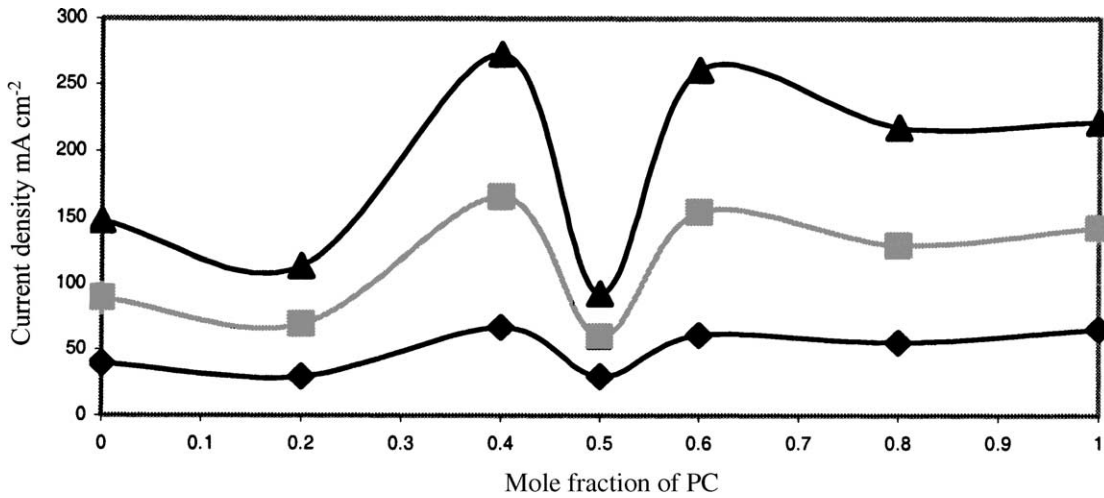

Fig. 14. Current density vs. mole fraction of PC of mixed carbon at 333 K at several voltages using 0.7 mg cm^{-2} of platinum: (◆), 700 mV; (■), 500 mV; (▲), 300 mV.
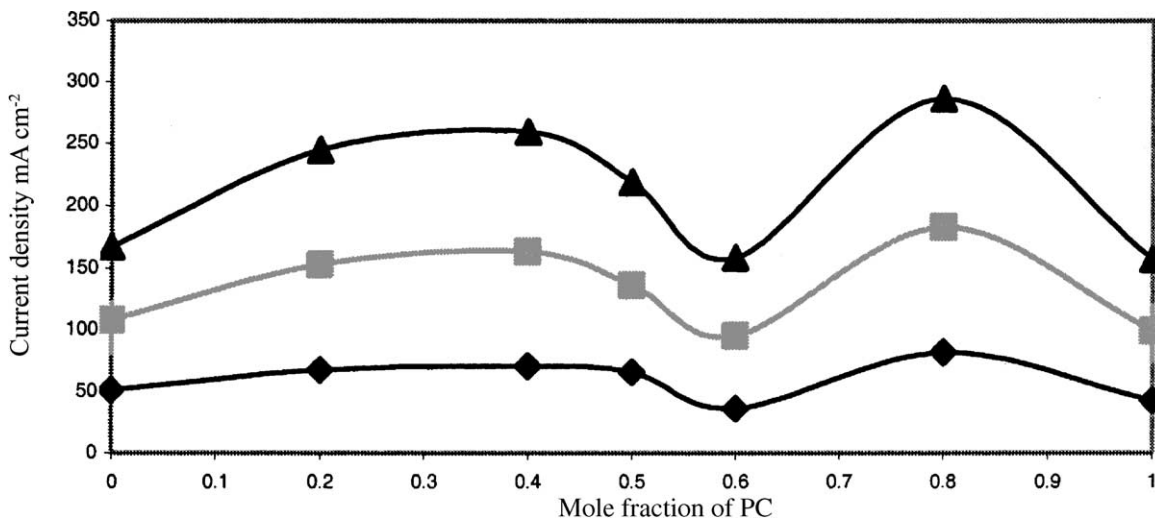

Fig. 15. Current density vs. mole fraction of PC at 333 K several voltages using 0.9 mg cm^{-2} of platinum: (◆), 700 mV; (■), 500 mV; (▲), 300 mV.
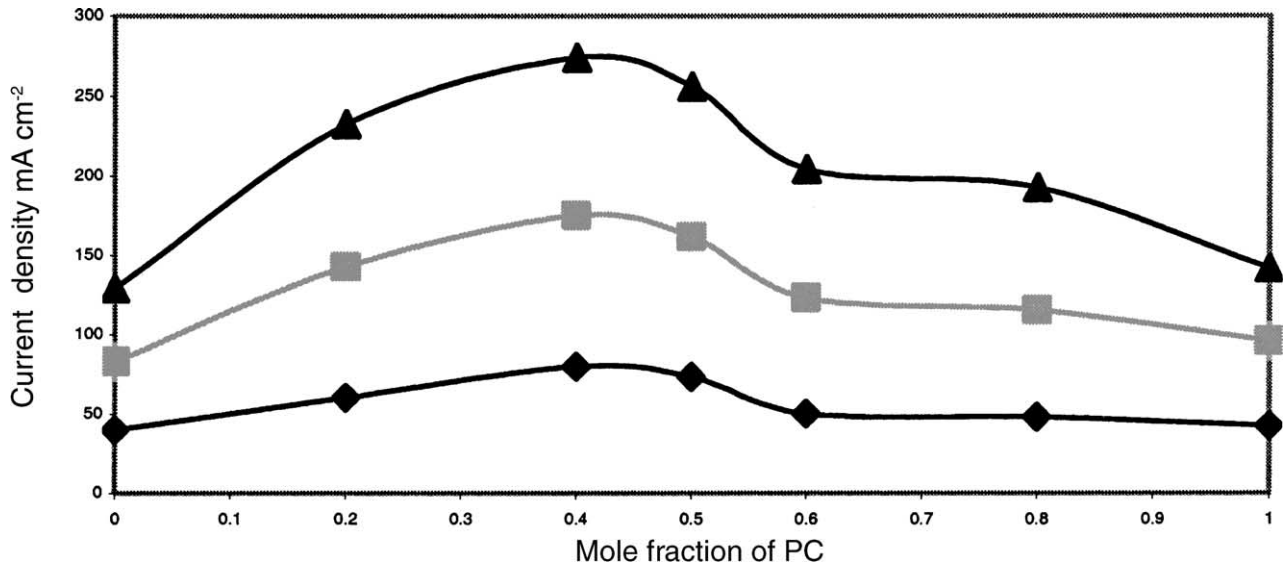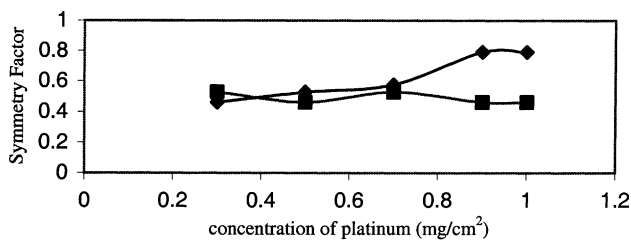
Fig. 16. Current density vs. die mole fraction of PC of mixed carbons at 333 K at several voltages using 1 mg cm^{-2} of platinum: ($\blacklozenge$), 700 mV; ($\blacksquare$), 500 mV; ($\blacktriangle$), 300 mV.

Fig. 17. Symmetry factor against concentration of platinum at 333 K: ($\blacklozenge$), platinum on carbon; ($\blacksquare$), platinum on activated charcoal.

Fig. 17. In the case of PAC, α is approximately constant. By contrast, the symmetry factor of the PC system changes from 0.5 to 0.8 as the amount of platinum is increased from 0.3 to 1 mg cm^{-2}. In the rate-determining step, since the amount of loaded platinum on PC is more than 0.7 mg cm^{-2}, the ORR has irreversible kinetics, where the ORR on PAC has reversible kinetics independent of the amount of platinum loaded in the reaction layer.
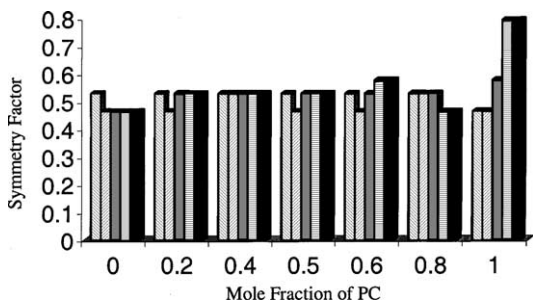

Fig. 18. Symmetry factors vs. mole fraction of platinum on carbon with various amounts of electrocatalyst at 333 K: ($\boxed{\diagdown}$), 0.3 mg cm^{-2}; ($\boxed{\diagup}$), 0.5 mg cm^{-2}; ($\blacksquare$), 0.7 mg cm^{-2}; ($\boxed{\equiv}$), 0.9 mg cm^{-2}; ($\blacksquare$), 1 mg cm^{-2}.

The symmetry factors for systems with various mole fractions and a range of platinum loading are given in Fig. 18. In all cases, with the exception of the pure PC system, the symmetry factor is around 0.5 and, consequently the ORR is reversible. It is concluded that at high loading of platinum, the reversibility of the ORR is due to synergetic effects arising from the presence of a physical mixture of the types of electrocatalyst in the reaction layer in a mole ratio between 0.2 and 0.8. The results presented here show that the strength of the synergetic effect depends on the amount of platinum in the reaction layer and the composition of the electrocatalyst.

4. Conclusions

In the present study, GDEs are fabricated in two stages: pressure processing followed by temperature processing. This novel construction methodology produces GDEs with higher current densities than those previously attained using GDEs constructed by means of simultaneous pressure and temperature processing. These results indicate the optimized operation of GDE is related to the fast kinetics of the ORR. The observation of high current densities and symmetry factors confirm this conclusion. Sampled dc voltammetry and a half-cell measurement apparatus have been used to determine the kinetic parameters of the ORR.

GDEs fabricated at low pressure gave superior ORR efficiency. The ORR shows a regular change in kinetics parameters (symmetry factor and exchange current density) when the GDE is fabricated at low pressure; an increase in the symmetry factor causes a decrease in exchange current density. A GDE with 30% PTFE in the reaction layer fabricated at a pressure of 60 kg cm^{-2} gives the best
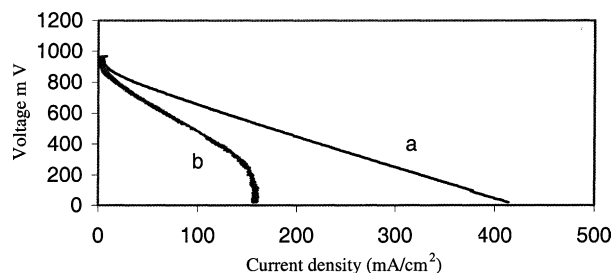
Fig. 19. Polarization curve for rate-determining step of ORR at 1 mg cm^{-2} loading of platinum electrocatalyst: (a) mixed carbon with 0.4 mole fraction of platinum on carbon; (b) platinum on carbon.

performance, with reversible ORR and fast kinetics being observed.

Physical mixtures of platinum electrocatalysts with different surface areas are found to enhance synergetically the catalytic performance in terms of both the voltage and current of the GDE. This synergism had two valuable consequences, it eliminates polarization concentration (Fig. 19) and gives rise to reversible ORR kinetics. Future work should be undertaken to understand and control the concerted electrocatalytic actions of carbon surfaces.

This is the first report of physical mixtures of electrocatalysts with different surface areas having a synergetic effect on the ORR. To observe the synergism, the correct mixture of electrocatalyst should be prepared. For example, at a platinum loading of 0.3 mg cm^{-2}, the maximum efficiency appears at a mole fraction of PC of 0.8, whereas at a platinum loading of 0.5 mg cm^{-2} the maximum value appears at a mole fraction of PC of 0.5.

Acknowledgements

References

[1] J. Appleby, Assessment of research needs for advanced fuel cells, Energy Int. J. 11 (1/2) (1986) 13–94.

[2] E. Barendrecht, Electrochemistry of fuel cells, in: L.J.M.J. Blomen, M.N. Mugerwa (Eds.), Fuel Cell Systems, Plenum Press, New York, 1993, pp. 73–119.

[3] J.H. Hirschenhofer, D.B. Stauffer, R.R. Engleman, M.G. Klett, Fuel Cell Handbook, Fourth ed., Parsons, Oxford, 1998.

[4] J. Larminie, A. Dicks, Fuel Cell Systems Explained, Wiley, New York, 2000.

[5] M. Uchida, Y. Aoyama, N. Eda, A. Ohta, J. Electrochem. Soc. 142 (1995) 463.

[6] H. Gharibi, M. Jalili, T. Rajabi, Colloid Surf. Int. J. 175 (2000) 361.

[7] H. Gharibi, B.M. Razavizadeh, M. Hashemianzahed, Colloid Surf. Int. J. 174 (2000) 373–375.

[8] H. Gharibi, M. Hashemianzahed, B.M. Razavizadeh, Colloid Surf. 196 (2000) 31–38.

[9] H. Gharibi, M.A. Safarpoor, A.A. Rafati, J. Colloid Interface Sci. 219 (1999) 217–224.

[10] H. Gharibi, A.A. Rafati, Langmuir 14 (1998) 2191–2196.

[11] H. Gharibi, B.M. Razavizadeh, A.A. Rafati, Colloid Surf. 136 (1998) 123–132.

[12] M. Shamsipur, N. Alizadeh, H. Gharibi, M. Mousavi, J. Chin. Chem. Soc. 44 (1997) 9–15.

[13] H. Gharibi, N. Alizadeh, M. Shamsipur, Bull. Chem. Soc. (Japan) 69 (1996) 311.

[14] N. Alizadeh, H. Gharibi, M. Shamsipur, Bull. Chem. Soc. (Japan) 68 (1995) 730–733.

[15] R. Palepu, H. Gharibi, D.M. Bloor, E. Wyn-Jones, Langmuir 9 (1993) 110–112.

[16] H. Gharibi, R. Palep, D.M. Bloor, O.G. Hall, E. Wyn-Jones, Langmuir 8 (1992) 782–787.

[17] W.-C. Lu, H. Chang, J. Phillips, J. Catal. 146 (1994) 608.

[18] H. Chang, J. Phillips, Langmuir 12 (1996) 2756.

[19] W.C. Conner Jr, G.M. Pajonk, S. Teichner, J. Adv. Catal. 34 (1986) 1.

[20] P.A. Sermon, G.C. Bond, Catal. Rev. 8 (1993) 211.

[21] L.-T. Weng, B. Delmon, Appl. Catal. A 81 (1992) 141.

[22] D. Bianchi, G.E.E. Gardes, G.M. Pajonk, S.J. Teichner, J. Catal. 38 (1975) 135.

[23] R.J. Willey, S.J. Teichner, G.M. Pajonk, J. Mol. Catal. 77 (1992) 201.

[24] P.A. Sermon, G.C. Bond, J. Chem. Soc. Faraday Trans. 1 72 (1976) 730.

[25] W.C. Conner Jr., G.M. Pajonk, S.J. Teichner, Adv. Catal. 34 (1986) 1–79.

[26] S. Mukerjee, J. Appl. Electrochem. 20 (1990) 537.

[27] L.J. Hillebrand, J.W. Lacksonen, J. Electrochem. Soc. 112 (1965) 249.

[28] J. Escard, C. Leclere, J.P. Contour, J. Catal. 29 (1973) 31.

[29] V.S. Bogotski, A.M. Snudkin, Electrochem. Acta 9 (1984) 757.

[30] N.M. Markovic, P.N. Ross, in: A. Wieckowski (Ed.), Interfacial Electrochemistry: Theory, Experiment and Applications, Marcel Dekker, New York, 1999, pp. 521–841.

[31] N.M. Markovic, R.R. Adzic, B.D. Cahan, E.B. Yeager, in: Proceedings of the ISI, Montreux, 1991, p. 138.

[32] N.M. Markovic, R.R. Adzic, B.D. Cahan, E.B. Yeager, J. Electroanal. Chem. 77 (1994) 249.

[33] F. El Kadiri, R. Faure, R. Durand, J. Electroanal. Chem. 301 (1991) 177.

[34] H. Kita, Y. Gao, K. Ohnishi, Chem. Lett. (1994) 73.

[35] N.M. Markovic, H.A. Gasteiger, P.N. Ross, J. Phys. Chem. 100 (1996) 6715.

[36] R.R. Adzic, in: J. Lipkowski, P. Ross (Eds.), Electrocatalysis, 1998 (Chapter 5).

[37] N.M. Markovic, H.A. Gasteiger, P.N. Ross, J. Electrochem. Soc. 114 (1997) 1591.

[38] B.N. Grgur, N.M. Markovic, P.N. Ross, Can. J. Chem. 75 (1997) 1465.

[39] N.M. Markovic, H.A. Gasteiger, B.N. Grgur, P.N. Ross, J. Electroanal. Chem. 467 (1999) 157.

[40] L. Qingfeng, H.A. Hjuler, N.J. Bje, Electrochim. Acta 45 (2000) 4219–4226.

[41] L.J. Bregoli, Electrochim. Acta 23 (1978) 489.

[42] M. Peuckert, T. Yoneda, R.A. Dalla Betta, M. Boudart, J. Electrochem. Soc. 133 (1986) 944.

[43] K. Kinoshita, J. Electrochem. Soc. 137 (1990) 845.

[44] R. Greef, R. Peat, L.M. Peter, D. Pletcher, J. Robinson, Instrumental Methods in Electrochemistry, Ellis Horwood/Wiley, New York, 1985.

[45] J.O.M. Bockris, S. Srinvasan, Fuel Cells: Their Electrochemistry, McGraw-Hill, New York, 1969.